Kuiper Belt Objects in the Planetary Region: The Jupiter-Family Comets

Stephen Lowry and Alan Fitzsimmons
Queen's University Belfast

Philippe Lamy
Laboratoire d'Astrophysique de Marseille

Paul Weissman
NASA Jet Propulsion Laboratory

Jupiter-family comets (JFCs) are a dynamically distinct group with low orbital inclinations and orbital periods ≤20 yr. Their origin has been shown computationally to be the Kuiper belt region beyond Neptune. Therefore studying the nuclei of these comets, as well as their coma species, can provide valuable insights into the nature of the kilometer-sized Kuiper belt objects (KBOs). These include their size distribution, internal structure, and composition, as well as some hints at their likely surface features. Although JFCs are much closer to the Sun than KBOs, they are still very difficult to observe due to their intrinsic faintness and outgassing comae. However, observational studies are advancing rapidly and we are now starting to place valuable constraints on the bulk physical properties of these nuclei. In this chapter, we review some of the more important findings in this field and their relevance to KBO studies.

1. KUIPER BELT OBJECTS: PROGENITORS OF THE JUPITER-FAMILY COMETS

Considerable progress has been made in understanding the dynamical histories of the low-inclination ecliptic comets (ECs) (*Duncan et al.,* 2004). It is generally accepted that most if not all of the ECs, consisting of the Jupiter-family comets (JFCs), Encke-type comets, and Centaurs, must have originated from the Kuiper belt. Indeed, it was dynamical studies of JFCs (*Fernández,* 1980; *Duncan et al.,* 1988) that suggested that the most efficient source for them was a low-inclination reservoir beyond the giant planets, in order to match the low-inclination distribution of the JFC orbits. These results then stimulated the first confirmed Kuiper belt object discovery (*Jewitt and Luu,* 1993; see also chapter by Davies et al.) after Pluto and Charon. Kuiper belt objects (KBOs) can be perturbed into Neptune-crossing orbits or out of stable resonances by gravitational interactions with the giant planets, collisions, or perhaps by nongravitational forces due to surface outgassing. Once this happens the KBOs can be handed down through the giant planets region toward the terrestrial planets zone (*Horner et al.,* 2004) and end up as JFCs.

Jupiter-family comets have orbital periods ≤20 yr, and low-inclination, direct orbits. Their orbital behavior is chaotic due to strong gravitational interactions with Jupiter, hence their name. Their aphelia are generally around 5–6 AU from the Sun, although some can eventually evolve to orbits entirely within the orbit of Jupiter, such as Comet 2P/Encke. Encke-type comets are simply old JFCs, and are treated as JFCs for the purposes of this review. Jupiter-family comets are defined by their dynamical Tisserand parameter T_J (with respect to Jupiter), which is conserved in the circular restricted three-body problem, and can provide a measure of the relative velocity of approach to Jupiter. T_J is defined as

$$T_J = \frac{a_J}{a} + 2\cos(i)\sqrt{(1 - e^2)a/a_J} \qquad (1)$$

where a, e, and i are the comet's orbital semimajor axis, eccentricity, and inclination, respectively, and a_J is the orbital semimajor axis of Jupiter. Jupiter-family comets are defined as those comets having $2 < T_J < 3$. Dynamical studies by *Levison and Duncan* (1994) found that T_J does not vary substantially for JFCs, i.e., only ~8% of comets moved in or out of this dynamical class throughout the computer simulations. Thus, the JFCs are dynamically distinct.

Recent dynamical studies have shown that the most likely source for most of the JFCs is the scattered disk objects (SDOs) (*Duncan and Levison,* 1997; see chapter by Gomes et al.). Scattered disk objects are in orbits with perihelia close to Neptune, and are actively interacting dynamically with that planet. This leads to a much higher probability that the SDOs will be thrown into the planetary region, as compared with classical KBOs (CKBOs), which are in more distant and stable orbits. The source of the SDOs is

likely objects from the inner Kuiper belt, close to Neptune, and remnant icy planetesimals from the Uranus-Neptune zone.

The importance of collisions in moving small KBOs into the various dynamical resonances has been discussed by *Stern* (1995) and *Farinella and Davis* (1996). Collisions play an important role particularly at diameters <20 km. In fact, as noted in these papers, most of the observed JFCs are likely collisional fragments from the Kuiper belt and thus may not represent the primordial state of the smallest, kilometer-sized end of the size distribution beyond Neptune. Whether primordial or not, studying the small KBOs and their collisional products is valuable for understanding formation and evolution in this size regime, and their thermal histories. As a daughter population of the KBOs, the JFCs provide a unique data source for understanding the physical properties of their progenitors.

As noted above, the JFCs are one of several dynamically distinct groups of comets in the solar system. The other major groups are the long-period comets (LPCs) and the Halley-type comets (HTCs). Long-period comets have orbital periods >200 yr (and up to ~10^7 yr) and have random orbital inclinations as well as very high eccentricities. Dynamical simulations place their likely formation zone in the giant planets region, from which they were scattered out of the planetary region to form the distant Oort cloud. The Oort cloud consists of ~10^{12} comets in gravitationally bound but very distant orbits, with semimajor axes between ~3000 and 100,000 AU. Occasionally, Oort cloud comets are perturbed back toward the planetary region where they appear as LPCs. Approximately one-third of observed LPCs are on their first return to the planetary region. Halley-type comets have orbital periods $20 < P < 200$ yr. Their orbits are more inclined than JFCs but not totally randomized like the LPCs, and have eccentricities also between that of the JFCs and LPCs. Their source region is not determined but they are likely a mix of Oort cloud and Kuiper belt comets, the latter again showing a preference for SDOs.

Recently, several objects with comet-like tails have been found in stable, low-inclination orbits in the outer asteroid belt, referred to as main-belt comets (MBCs) (*Hsieh and Jewitt,* 2006). All three members of this group are associated with the Themis collisional family at ~3.16 AU, and therefore are likely to be volatile-rich asteroids, where volatiles buried beneath the surface have been exposed by recent impacts. The relatively stable orbits of these objects suggest that they formed at their current location in the outer asteroid belt, and thus they have little or no connection with the JFCs or the Kuiper belt.

Jupiter-family comets are the most observationally accessible of the comet groups, with perihelion distances in the realm of the terrestrial planets, and relatively short periods that result in frequent and predictable returns. They are typically much "older" than LPCs (which make an average of only five returns) (*Weissman,* 1979), having likely been in their current orbits for many hundreds of returns or more. This has the advantage that their surfaces are less active, allowing the nucleus to be observed directly in many cases. However, it also means that the observed surfaces are now substantially evolved from their presumably primitive state in the Kuiper belt.

Given our extensive knowledge of JFCs, which comprise more than 200 known objects, it is impossible to provide a complete, detailed description of the properties of this population in a single chapter. For indepth discussions on numerous aspects of the JFCs, we refer the reader to the comprehensive reviews by *Lamy et al.* (2004), *Weissman et al.* (2004), *Samarasinha et al.* (2004), and *Bockelée-Morvan et al.* (2004), among many others, in the recent *Comets II* book. Instead, we focus herein on the broad ensemble properties of both JFCs and KBOs. We make comparisons that offer insights into the nature of the parent KBOs, such as their likely size distribution at kilometer sizes, discussed in section 2. The JFC population is currently unobservable from Earth, so provide a valuable proxy for understanding the nature of the KBO size distribution at diameters <20 km. If the KBOs are the parent bodies of JFCs then it is reasonable to suggest that their internal structures are very similar (with the exception of larger KBOs where gravity dominates their internal structure). Information on internal structure can be inferred from the rotational properties of JFC nuclei (section 3), using methods similar to those developed to study the asteroid population.

Surface imaging of JFC nuclei obtained by recent spacecraft flybys is potentially very powerful in providing representative, closeup views of the surfaces of KBOs. However, we must also recognize that comet nucleus surfaces have likely been modified from their initial state in the Kuiper belt by processes such as sublimation and space weathering (section 4). Some KBOs are active, displaying visual comae, and JFCs may provide clues to understanding this activity, although the volatiles involved are likely very different, given the substantially different thermal regimes in which they occur. In this regard, other cometary populations, in particular the LPCs, may provide more valuable insights as the LPCs often display activity at relatively large solar distances. Jupiter-family comets are particularly valuable for understanding the potential future evolution of KBO surfaces when they are perturbed out of the Kuiper belt toward the terrestrial planets region (section 4). The proximity of JFCs allows for much easier study of outflowing comae, and thus their molecular composition. This is covered in section 5.

The study of cometary nuclei is rapidly advancing and data on their physical properties continues to grow, in some cases well beyond the scope of the *Comets II* reviews mentioned previously. As well as utilizing ever-larger ground-based telescope facilities, the Hubble Space Telescope (HST) has proved most fruitful in probing cometary nuclei, given the high spatial resolution that allows for better coma-removal during nucleus imaging. Additionally, the NASA Spitzer Space Telescope is opening up new areas of inves-

tigation through its ability to study cometary nuclei and comae in the infrared.

2. PROBING THE KUIPER BELT SIZE DISTRIBUTION AT THE KILOMETER SIZE RANGE

Jupiter-family comets have typical nucleus radii of 1–5 km. Thus, they are smaller than any detected KBOs. Since it is largely agreed that the JFCs derive primarily from the KBO region, including the high-inclination scattered disk population, the JFCs provide a ready means of sampling both the size distribution and physical nature of small KBOs.

Size estimates for cometary nuclei have always been difficult to obtain. When the comets are in the terrestrial planets region and close to Earth, they are active, and their bright comae obscure the signal from their relatively small, dark nuclei. When the comets are far from the Sun and presumably inactive, they are faint objects, with typical apparent magnitudes $m_R \geq 22$, and require large-aperture telescopes to observe them.

A variety of techniques are used to estimate the sizes of cometary nuclei. These include (1) direct imaging by spacecraft; (2) simultaneous optical and IR photometry of a distant or low-activity nucleus that permits a solution for both the size and albedo; (3) IR photometry alone of a distant or low-activity nucleus, where it can be assumed that almost all sunlight incident on the low-albedo object is re-radiated as thermal energy; (4) HST imaging of comets close to Earth with modeling and subtraction of the coma signal; (5) CCD photometry of distant nuclei, far from the Sun where they are likely to be inactive, and using an assumed albedo of typically 4%; and (6) radar imaging. Of these techniques, (5) is the most widely used, followed closely by (4). Although both techniques rely on an assumed albedo, the repeatability of observed nucleus absolute magnitudes by numerous observers, as well as the confirmation of size and shape estimates from flyby spacecraft, show that they are indeed reliable. Flyby spacecraft have only imaged four cometary nuclei to date: 1P/Halley in 1986 (Giotto, Vega), 19P/Borrelly in 2001 (Deep Space 1), 81P/Wild 2 in 2004 (Stardust), and 9P/Tempel 1 in 2005 (Deep Impact).

There are generally two types of observations: snapshot and lightcurve. Snapshot observations are comprised of several exposures of a nucleus taken in quick succession. They capture the brightness of the nucleus at an instant in time, but there is no knowledge of where the images are in the rotation lightcurve of the presumably irregularly shaped nucleus. More complete coverage is provided by lightcurve observations that image the nucleus over many hours, and even on several successive nights, or orbits in the case of the HST and the Spitzer Space Telescope. This much more complete temporal coverage allows one to obtain the rotation period of the nucleus, and a lower limit on its axial ratio.

An important question in observing distant nuclei is the possible presence of coma. The observer's goal is to image the bare nucleus with no coma contamination of the signal. To do this, cometary targets are usually chosen when they are far from the Sun, beyond 3 AU (preferably >4 AU), and on the inbound leg of their orbits. Many JFCs display more activity postperihelion on the outbound legs of their orbits, even beyond 3 AU where water ice sublimation in theory becomes negligible. A technique to check for coma contamination is to compare the image profile of the nucleus to that of nearby stars in the field. The coma will make itself known as a widening of the comet's radial brightness profile as compared to the on-chip background stars. If the nucleus appears stellar then the likelihood of significant coma contamination is fairly minimal.

The success of these techniques is demonstrated by the repeatability of nucleus size estimates by multiple observers, and by comparison with direct imaging in the four cases where comets have been encountered by spacecraft. For example, *Weissman et al.* (1999) and *Lamy et al.* (2001) found dimensions for the nucleus of 9P/Tempel 1 of 3.8 × 2.9 km and 3.9 × 2.8 km, respectively, each assuming an albedo of 0.04. The dimensions derived from the Deep Impact flyby in 2005 are 3.8 × 2.5 km with a measured albedo of 0.04 (*A'Hearn et al.,* 2005), in excellent agreement.

An important quantity to estimate is the slope of the cumulative size distribution, which can be expressed as a power law of the form

$$N(>r) \propto r^{-\alpha} \quad (2)$$

where r is the radius, N is the number of nuclei with radius >r, and α is the slope parameter. The cumulative brightness distribution can similarly be expressed by an equation of the form

$$N(<H) \propto 10^{\beta H} \quad (2)$$

where H is the absolute magnitude, N is the number of nuclei with absolute magnitude <H, and β is the slope parameter. For populations with the same albedo, the two equations are related by $\alpha = 5\beta$.

Several groups have assembled size estimates of cometary nuclei and derived the size distribution. *Weissman and Lowry* (2003) compiled a catalog of CCD, IR, HST, and spacecraft measurements of the dimensions of cometary nuclei. The catalog presently contains 120 measurements of 57 JFCs and 4 HTCs. The data were normalized to an assumed albedo of 0.04 except in cases where the albedo was directly measured. Weissman and Lowry found that the cumulative number of JFCs at or larger than a given radius can be described by a power law with a slope parameter of $\alpha = 1.73 \pm 0.06$ (Fig. 1) for nuclei with radii between 1.4 and 6 km. This corresponds to $\beta = 0.35 \pm 0.01$.

As seen in Fig. 1, the cumulative size distribution has two parts: a steeply ascending series of points that is fitted to give the slope parameter, followed by a roll-off at smaller sizes that is indicative of observational incompleteness. The

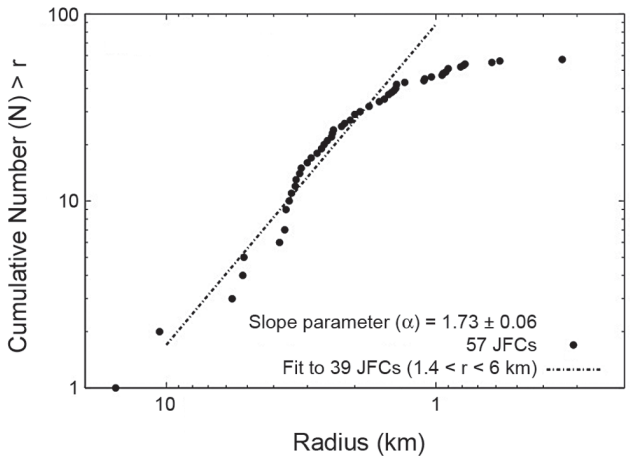

Fig. 1. One of several size distribution estimates for JFCs (*Weissman and Lowry,* 2003). Current estimates of the slope of this distribution are much shallower than for large KBOs, which we believe is reasonable evidence for a broken power-law size distribution within the Kuiper belt.

choice of the lower limit for the fitting of the size distribution has a strong effect on the value of the fitted slope. Since about one-fourth of all JFC nuclei have had size estimates to date, it is difficult to estimate at what size the determination of the distribution is complete. This is illustrated by *Meech et al.* (2004), who found a slope value of $\alpha = 1.91 \pm 0.06$ for JFC nuclei with radii between 2 and 5 km, but a shallower slope of $\alpha = 1.45 \pm 0.05$ for nuclei with radii between 1 and 10 km. *Lamy et al.* (2004) found a slope parameter $\alpha = 1.9 \pm 0.3$ for nuclei larger than 1.6 km in radius. *Lowry et al.* (2003) found a slope of $\alpha = 1.6 \pm 0.1$. These values correspond to $\beta = 0.29$–0.38.

In contrast to the three groups cited above, *Fernández et al.* (1999) and *Tancredi et al.* (2006) found much steeper values of $\alpha = 2.65 \pm 0.25$ and $\alpha = 2.7 \pm 0.3$ ($\beta = 0.53$ and 0.54), respectively, for nuclei brighter than H = 16.7, corresponding to a radius of ~1.7 km. The inclusion of uncalibrated magnitudes reported in the Minor Planet Circulars may seriously compromise their sample and thus contribute to the differences in slope parameter. However, even if these higher values of α are correct, it is clear that the slope of the JFC size distribution is shallower than similar estimates for the larger KBOs.

Weissman and Lowry (2003) pointed out that the size distribution estimate for JFCs was probably not the primordial size distribution when these nuclei first evolved inward from the Kuiper belt. Sublimation mass loss and fragmentation events have likely decreased the sizes of the nuclei over time. Because sublimation loss is a surface process and thought to be independent of nucleus radius, Weissman and Lowry estimated that smaller nuclei would proportionately lose a greater fraction of their initial radius over time than larger nuclei. They estimated that due to this effect the primordial slope α of the cumulative size distribution would be ~0.1 greater than the currently estimated values. Thus, based on the work of Weissman and Lowry, *Meech et al.* (2004), and *Lamy et al.* (2004), the primordial slope parameter likely has a value between 1.83 and 2.01.

Early theoretical estimates of the slope parameter were largely based on *Dohnanyi* (1969), who showed that for constant material strength vs. size, the cumulative size distribution of a collisionally evolved population should have a slope of $\alpha = 2.5$. However, we now know that strength is a function of size (e.g., *Asphaug et al.,* 2002). *O'Brien and Greenberg* (2003) applied current strength models to show that the expected cumulative slope parameter α in the gravity-dominated regime for a collisionally evolved population is 2.04. This is similar to the shallower values cited above, and also to the value found for near-Earth objects of $\alpha = 1.96$ (*Stuart,* 2001) ($\beta = 0.39$).

We can compare the brightness distribution of JFCs with that of KBOs. In the case of the KBOs, the estimated quantity is the slope of the cumulative luminosity function (CLF), which is defined in terms of apparent magnitudes but can be related to the KBO size distribution, and compared with other populations, if several assumptions are applied (see chapter by Petit et al.). Typical KBO β values range from 0.63 to 0.69 (*Trujillo et al.,* 2001; *Gladman et al.,* 2001; *Bernstein et al.,* 2004). Note that a more accurate comparison could be made if the KBO distribution employed absolute magnitudes, as is done for the JFCs. The shallower slope parameter of the JFCs, which are considerably smaller than the observed KBOs, is likely due to a change in the slope of the KBO size distribution at smaller sizes (*Weissman and Levison,* 1997; *Bernstein et al.,* 2004). Barring any unusual processes that would sharply change the size distribution of small KBOs as they evolve inward to JFC orbits, the size distribution of the JFCs can be considered as reasonable proof that the KBO size distribution must be much shallower at smaller sizes. *Sheppard et al.* (2000) found a CLF slope for Centaurs of 0.6 ± 0.1, consistent with the CLF for the KBOs. Thus, the break in the KBO size distribution likely occurs at radii lower than the faintest detected Centaurs, which is about 10–20 km.

3. ROTATION PROPERTIES, BULK DENSITY, AND INTERNAL STRUCTURE

Rotational properties of cometary nuclei are difficult to obtain. While being much closer than KBOs, the smaller size of the JFCs means that they are inevitably faint. When close to the Sun the nucleus is effectively shielded due to the presence of a masking coma, which acts to reduce the brightness amplitude of the rotational lightcurve should the modulation be detected at all.

As mentioned above, time-series photometric measurements can be made from which periodicities can be evaluated. The lightcurve amplitude is related to the elongation of the nucleus, and by combining this with the measured period, one can set limits on the nucleus density, i.e., the minimum density required in order to withstand centrifugal disruption under the assumption of negligible cohesive strength (*Luu and Jewitt,* 1992; *Weissman et al.,* 2004). The

density estimate is a lower limit because we use the projected axial ratio, a/b, which is a lower limit to the true axial ratio since the orientation of the rotation axis is unknown. Also, the nucleus does not necessarily need to be spinning at its rotational disruption limit. Lightcurves for ~22 JFC nuclei have been obtained to date (Fig. 2). The derived rotation periods range from ~5.2 to 40.8 h, while the projected axial ratios range from 1.02 to 2.60. The inferred, lower-limit nucleus bulk densities are given by the position of each comet in the figure and are limited to ≤0.56 g cm^{-3}, consistent with density values determined through other methods (*Weissman et al.,* 2004).

Lowry et al. (2003) also noted that a 5.2-h cutoff in rotation period exists for cometary nuclei, corresponding roughly to a density cutoff of 0.6 g cm^{-3}. As more comet data is acquired that result seems to be holding up quite well. A similar spin-period cutoff is unambiguously seen for the asteroid population, albeit for a much larger sample, at the faster period of 2.2 h and thus higher density of ~2.5 g cm^{-3} (see *Pravec et al.,* 2002). Pravec et al. interpret this result as evidence for small asteroids being loosely bound, gravity-dominated aggregates with negligible tensile strength. The same description should then apply to JFCs. There exists a distinct population of small (<150 m) asteroids that can spin well above this limit, believed to be monolithic-rock fragments, perhaps individual fragments of larger rubble-pile asteroids.

Figure 2 compares all cometary lightcurve data with those available for KBOs and Centaurs. Cometary nuclei are shown as open circles, Centaurs as filled triangles, and KBOs as filled circles. One can see that the rotation period vs. shape distributions overlap quite nicely, with exceptional objects labeled. It is thus reasonable, even at this early stage,

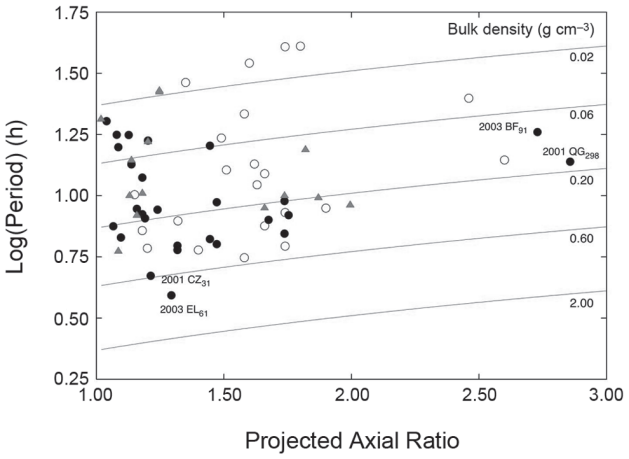

Fig. 2. Available cometary nucleus lightcurve data (*Snodgrass,* 2006). Comet data are shown as open circles, KBOs as filled circles, and Centaurs as filled triangles. KBO and Centaur data are from *Lacerda and Luu* (2006), *Trilling and Bernstein* (2006), *Ortiz et al.* (2006), and *Rabinowitz et al.* (2006). The distributions for JFCs and KBOs are similar on this plot. Like comets, KBOs all lie above the 0.6 g cm^{-3} threshold, with the exception of the large object 2003 EL$_{61}$. Curves are lines of constant density, for a simple centrifugal breakup model.

to apply a similar interpretation as done for the small asteroid population with regard to their rubble-pile internal structure. Further evidence for the rubble-pile structure of comets comes from their observed disruption, such as in the case of D/1999 S4 (LINEAR) and D/1993 F2 (Shoemaker-Levy 9). Further discussion on the likely internal structure of KBOs can be seen in the chapter by Coradini et al.

A cutoff density of ~0.6 g cm^{-3} implies that comets are remarkably porous (~70%) (*Snodgrass,* 2006) for nuclei with similar proportions of dust and ice to that found for 9P/Tempel 1 by Deep Impact. Snodgrass also points out that there is a trend for the fastest-rotating nuclei to have lower values of a/b, which may reflect the inability of the rubble-pile nuclei to maintain extended shapes near the rotational disruption limit, again similar to small asteroids and JFCs.

There is only one object that appears to be rotating faster that the proposed spin period cutoff at 5.2 h. That is the large object 2003 EL$_{61}$, which rotates at 3.9 h (*Rabinowitz et al.,* 2006). The presence of such a body should not necessarily rule out the rubble-pile interpretation of the available lightcurve data, but its existence requires highlighting. The higher density of this large object (~1500–2500 km in length) can likely be explained by gravitational compression. A major goal in the study of cometary nuclei is to populate the graph in Fig. 2, to build up a more robust picture of the rotation period distribution.

Alternatively, *Holsapple* (2003) has suggested that small cohesive strengths, on the order of 10^4 dynes cm^{-2}, could allow even fast-rotating, elongated asteroids to survive as rubble piles. This value is similar to the tensile strengths inferred for cometary nuclei, although these calculations do not explain the sharp edge seen for the vast majority of small asteroids in the rotation period vs. axial ratio plot of *Pravec et al.* (2002). The existence of that edge strongly implies that many of these bodies are indeed acting as if they are strengthless.

Analyzing the actual distribution of spin periods for JFCs may not reveal much information about the spin rate distribution of small KBOs as cometary spin rates can be modified. Outgassing can alter the period over timescales less than the orbital period. Other mechanisms are planet encounters or even the Yarkovsky-O'Keefe-Radzievskii-Paddack (YORP) effect (*Rubincam,* 2000). The YORP effect is a torque due to both incident solar radiation pressure and the recoil effect from the anisotropic emission of thermal photons on small bodies in the solar system. The effect was directly detected for the first time on near-Earth asteroid (54509) 2000 PH5 (*Lowry et al.,* 2007; *Taylor et al.,* 2007). However, YORP timescales are long compared with other period-changing mechanisms. The available lightcurve data for JFCs and KBOs show the rotation-period distributions to be flat (*Snodgrass,* 2006), expected for comets but not necessarily for KBOs, which should be similar to the observed collisionally relaxed Maxwellian distribution seen for asteroids. This implies that the spin rates of KBOs and JFCs are indeed being altered over time, although more data are required to confirm these preliminary results based on limited data.

4. SURFACE CHARACTERISTICS AND EVOLUTION OF JUPITER-FAMILY COMETS

4.1. The Search for Compositional Links to Kuiper Belt Objects from Colors and Albedos

Colors and albedos are important properties of solar system small bodies as they can constrain composition and surface processes. Common patterns or trends in these properties among KBOs and cometary nuclei could reveal information about their putative relationships and subsequent evolution. Broadband colors are not as diagnostic in terms of surface composition as spectroscopy, but systematic correlations between different color indices, and between color indices and dynamical parameters could suggest evolutionary trends or compositional groupings. Such groupings are seen in the asteroid population, which radically advanced our understanding of the nature of the asteroid belt (e.g., *Tholen,* 1984).

Several forms of color groupings in the Centaur and KBO populations have been reported. A color bimodality was reported within both populations by *Tegler and Romanishin* (1998) and *Tegler and Romanishin* (2003). However, after independent analysis of the same sample, *Peixinho et al.* (2003) put forward that if one separates the complete sample into Centaurs and KBOs, then the color bimodality exists only in the Centaur population, while the KBOs exhibit a continuous spread. More recent data from a large-scale homogeneous survey at the European Southern Observatory (ESO) imply the existence of a KBO compositional taxonomy (*Barucci et al.,* 2005; *Fulchignoni et al.,* 2006; see also chapter by Fulchignoni et al.). With this in mind, it is a major goal of cometary nucleus observers to search for potential compositional groupings or trends in JFC nuclei, to develop compositional links with KBOs, as only dynamical links have been firmly established so far.

Broadband color data is normally acquired over spectroscopic data simply because cometary nuclei are small and faint, as noted above, and sometimes can only be observed using CCD imaging techniques with broadband filters that effectively integrate the observed flux over a large wavelength range, which improves S/N substantially. Imaging over several bandpasses can result in a broadband spectrum. Cometary nucleus spectroscopy ideally requires 5–8-m-class telescopes to attain the required S/N to reveal surface compositional spectroscopic signatures. To date, cometary nuclei have been primarily observed using groundbased 3–4-m telescopes and the HST.

The following discussion of the comparison of colors between KBOs and cometary nuclei is based on two new extended treatments of this topic by *Lamy and Toth* (2005) and *Snodgrass* (2006) (hereafter *LT05* and *S06*, respectively). The former is based on a compilation of color indices for 282 KBOs and 35 nuclei of ECs, where the EC observations were carried out with the HST. The *LT05* EC sample includes both JFCs and Encke-types ($T_J > 3$, $a < a_J$). *S06* is based on their groundbased survey of cometary nuclei at large heliocentric distances. Although nucleus color data are still limited at present, these datasets are the largest homogeneous datasets of their kind. Therefore, conclusions drawn will naturally be on firmer footing than from just a collation of observations presented throughout the literature. In the following discussion we describe what is seen in the available data, and what this actually means for studying surface properties of the small KBOs and potential future evolutionary states.

4.1.1. The distributions of color. An important measurement is the color distribution of JFCs and how they compare to either the ensemble KBO color distribution, or that of various KBO dynamical subgroups. Figure 3 displays the histograms of the four color indices (B–V), (V–R), (R–I), and (B–R). The top row includes all KBOs, while the bottom row includes all ECs (excluding Centaurs). Both populations exhibit a large range of colors, in fact much larger for cometary nuclei than first anticipated by *Luu* (1993). However, there is a clear trend for KBOs to be globally redder than comets. A few objects bluer than the Sun exist in both populations, but we point out that, in the case of the nuclei, large uncertainties affect their indices so that they could well be less blue than implied by Fig. 3. This global perception hides a more diverse situation when considering the different dynamical classes of KBOs. To a large extent, the extreme red color comes from the classical KBOs in both low- and high-inclination orbits (CKBO-LI, CKBO-HI). The bimodality of the distribution of colors for the Centaurs [best seen on the (B–R) index] is suspected for Plutinos but is totally absent for comets, although the number of comet nucleus color measurements is small. The closest associations for the cometary nuclei based on the presently available distributions of colors (Fig. 3) would be the SDOs and the Centaurs, which interestingly are their most likely parent bodies based on dynamical studies (section 1).

The situation of the color-color correlations is highly contrasted among KBOs. There exists different partial correlations, i.e., involving only two color indices (e.g., Plutinos and Centaurs) with implications for the multiplicity of coloring agents and/or processes (*Peixinho et al.,* 2004; *Doressoundiram et al.,* 2005). The situation is radically different for cometary nuclei as a nonparametric statistical test using the Spearman rank correlation has indicated that there are no statistically significant correlations in the global set of colors (*LT05*). *S06* combined the available (V–R) and (R–I) data from the published literature with many of their own new measurements and found no color groupings and no evidence for the ultrared matter on JFC surfaces, as seen on KBOs (Fig. 4), consistent with *Jewitt* (2002) and *Delsante et al.* (2004). The mean (V–R) color index was found to be ~0.45 for the JFCs (from 31 measurements), as compared to ~0.59 for KBOs (based on 62 data points).

Also, *LT05* conducted systematic Komolgorov-Smirnov tests between the cumulative distributions (CDs) of color indices of the different populations. They found that the original CDs do not reveal compositional relationships between KBOs and ECs, as also noted by *Hainaut and Delsanti* (2002) and *Doressoundiram et al.* (2005). The highest probabilities come from the (B–V) index and favor first

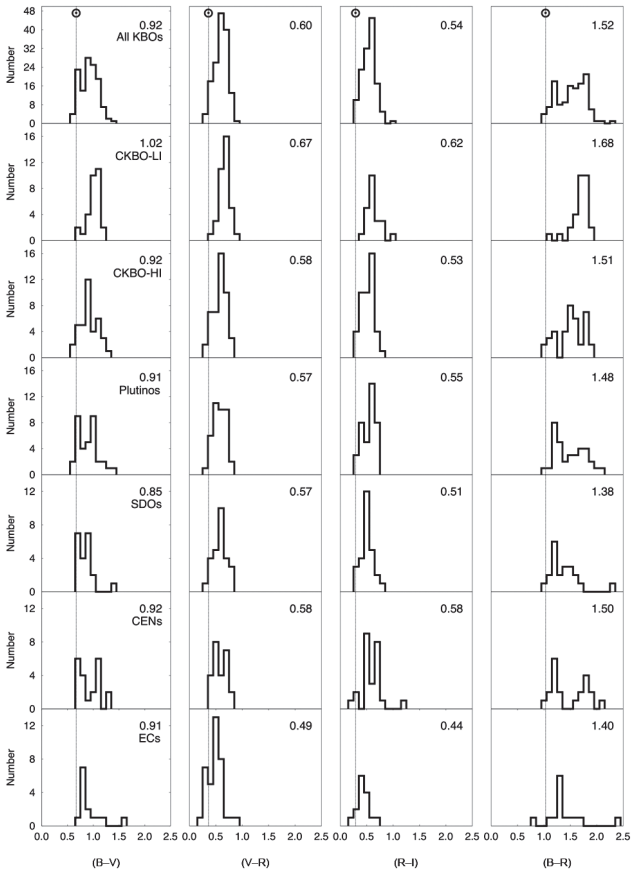

Fig. 3. Distributions of the color indices for different families of primitive bodies of the solar system: (B–V) (first column), (V–R) (second column), (R–I) (third column), and (B–R) (fourth column). From the top row to the bottom are all KBOs, the classical KBOs in low-inclination orbits, the classical KBOs in high-inclination orbits, the Plutinos, the scattered disk objects, the Centaurs, and finally the nuclei of ecliptic comets at the bottom. The means of the distributions are indicated. Solar colors are marked by vertical lines. Data are from *Lamy and Toth* (2005).

the Centaur–EC connection, followed by the SDO–EC and the Plutino–EC relationships, but these probabilities never exceed 42%. Color differences between the different families of primitive objects are most likely due to their formation and evolution at widely different places in the solar system. Considering the observed color distribution of Centaurs and ECs (and extinct cometary candidates within the asteroid population), ultrared matter has to be progressively removed or buried as these objects evolve toward the inner part of the solar system. *LT05* favor thermal alteration of different organic compounds because it can differentially affect the colors as observed.

4.1.2. Correlations between color, orbit, and size. It is also worthwhile investigating potential correlations between color and distance, as well as color vs. size. The case of the color-distance relationship is highly contrasted among the individual families of KBOs. On the basis of the analysis of *Peixinho et al.* (2004), the CKBOs do not show a color-semimajor axis relation. The larger objects do exhibit a strong correlation, with the colors increasing with semimajor axis and perihelion distance. In agreement with *Doressoundiram et al.* (2005), *Peixinho et al.* (2004) did not find any color-distance trend, neither for the SDOs nor for the Centaurs, contrary to *Bauer et al.* (2003), who found strong correlations of the (V–R) and (R–I) indices of Centaurs with semimajor axis. Regarding cometary nuclei, *LT05* have determined that (1) for the red nuclei, the (V–R) index appears to vary quasilinearly with perihelion distance while the other two indices do not, and (2) for blue nuclei, their colors are independent of perihelion distance. As for size, there now seems to be a consensus that the larger Plutinos are redder than the small ones (*Hainaut and Delsanti,* 2002; *Peixinho et al.,* 2004). The case of CKBOs remains confused because of possible multiple correlations between colors and perihelion distances, inclinations, and sizes. Based on the present data, colors are uncorrelated with size for SDOs, Centaurs, and cometary nuclei. This was also the case for the *S06* cometary dataset.

4.1.3. Comparing the albedos of Kuiper belt objects and Jupiter-family comets. Kuiper belt objects show a remarkable diversity of albedos ranging from ~1% to larger than 70%, and this property applies among both small and large, and gray and red objects. In fact, there is currently no evidence of correlations between albedo and either object size, color, or dynamical properties (with the possible exception of orbital inclination) (*Grundy et al.,* 2005). Cometary nuclei exhibit a very narrow range of albedos, ranging from ~3% to ~5% (*Lamy et al.,* 2004) so that a canonical value of 4% can be safely applied to derive sizes from magnitudes, contrary to KBOs. Asteroids in comet-like orbits, many of which are thought to be extinct comet candidates, are also very dark with albedos as low as 2% (*Fernández et al.,* 2001). Figure 5 displays the distribution of albedos of

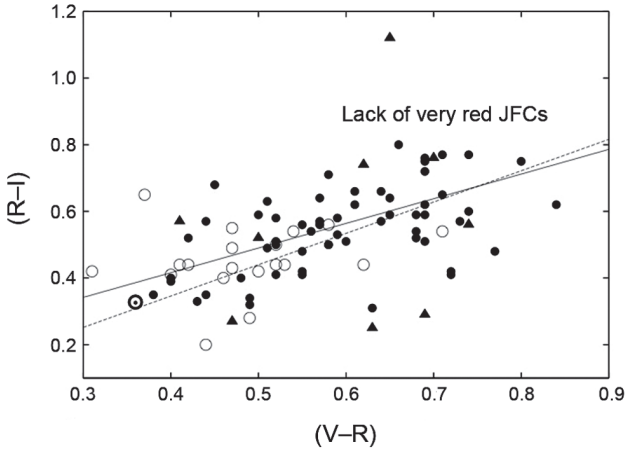

Fig. 4. (R–I) vs. (V–R) for all JFCs, KBOs, and Centaurs with known colors. Open circles = JFCs; filled circles = KBOs; filled triangles = Centaurs. The position of the Sun on these axes is marked. The solid line shows the best fit to the comet data; the dashed line is the fit to the KBOs. KBO and Centaur data from *Jewitt and Luu* (2001) and *Peixinho et al.* (2004). From *Snodgrass* (2006).

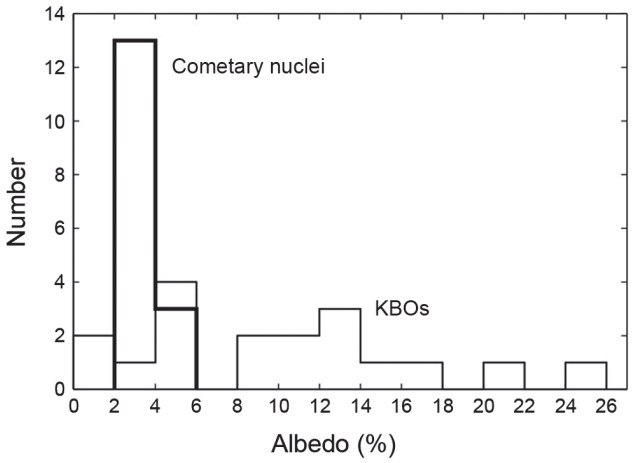

Fig. 5. Distributions of albedo (V- and R-band values combined) for the KBOs and cometary nuclei. Data from *Lamy et al.* (2004) and chapter by Stansberry et al.

KBOs (see chapter by Stansberry et al.) restricted to ≤30%, and of cometary nuclei as compiled by *Lamy et al.* (2004) augmented by the recent result of *Fernández et al.* (2006) for Comet 162P/Siding-Spring. For the present purpose of illustrating the widely different behaviors, we have merged V- and R-band determinations.

The colors and albedos of primitive bodies of the solar system result from their intrinsic initial composition (which may vary with their place of formation in the protoplanetary nebula) and many competing processes that subsequently alter their surfaces like collisional erosion and cratering, thermal processes such as volatile transport or differentiation, radiolysis and photolysis aging, impact by micrometeroids, and mantling from either impact ejecta or cometary activity. The dependence of collisional erosion rates upon size and orbital parameters (inclination and eccentricity) is often invoked to explain the diversity of albedos among KBOs since more pristine subsurface materials are expected to be brighter than space-weathered surfaces. Such a process is absent for cometary nuclei, and that may explain their narrow range of albedos. Alternatively, KBOs may possess surface frosts, which simply do not survive the journey to the planetary region.

4.2. Surface Morphology from Spacecraft Flybys

The four cometary nuclei observed to date by flyby spacecraft show vastly different shape and surface morphologies, although this may be due in part to the different spatial resolutions of the imagery for each nucleus (Fig. 6). Comet 1P/Halley's nucleus most clearly appears to be a rubble-pile structure, with large topographic features and, at least, a binary shape. About 30% of the illuminated surface is active, with large, apparently collimated jets (*Keller et al.,* 1986). The remainder of the surface is inactive and likely covered by a lag deposit crust of large particles that serve to insulate the icy-conglomerate material at depth.

The nucleus of 19P/Borrelly also has a binary shape but has a smoother surface with less topography and some evidence of erosional processes (*Soderblom et al.,* 2002). In addition to chaotic terrain, Borrelly displays mesa-like structures on its surface with smooth, flat tops and steep walls. It has been suggested that the walls of the mesas are where sublimation is currently taking place. In contrast to Halley, only a few percent of the nucleus surface appears active. Comet 81P/Wild 2 has a fairly ellipsoidal shape but a very unusual surface morphology, covered by numerous shallow and deep depressions that may be either eroded impact craters or sublimation pits, or some combination of the two (*Brownlee et al.,* 2004). Large blocks protruding from the surface also suggest an underlying rubble-pile structure. The orbital history of 81P/Wild 2 suggests that it may be a relatively young JFC, having been thrown into the terrestrial planets region after a close encounter with Jupiter in 1971, and thus the surface may preserve features that are truly

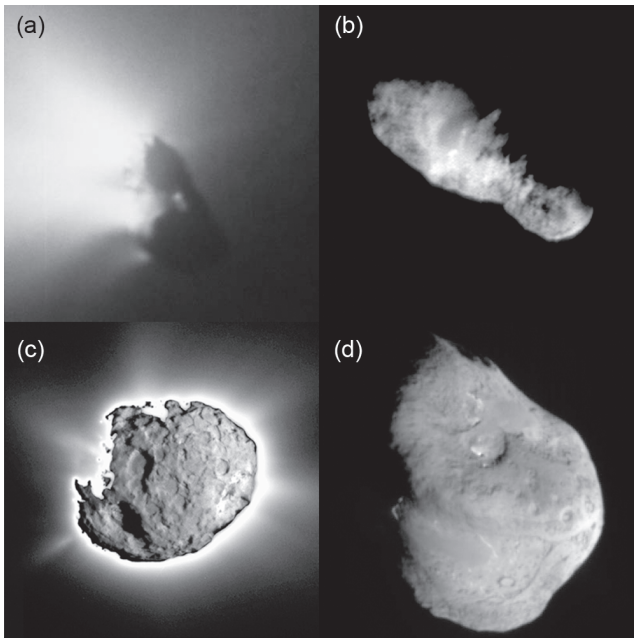

Fig. 6. There have been four cometary nuclei imaged through spacecraft flybys to date, with each flyby revealing very different surface features. Although many of these features could have resulted from evolutionary processes occuring after their departure from the Kuiper belt, clues to their internal structure and surface composition could mimic KBOs (see text). **(a)** Comet 1P/Halley from the Giotto encounter in 1986 (*Keller et al.,* 1986); **(b)** Comet 19P/Borrelly from Deep Space 1 taken in 2001 (*Soderblom et al.,* 2002); **(c)** Comet 81P/Wild 2 imaged in 2004 by the Stardust sample return mission (*Brownlee et al.,* 2004); **(d)** the most detailed images to date have come from the Deep Impact mission to Comet 9P/Tempel 1 in 2005 (*A'Hearn et al.,* 2005). Image credits: ESA/Max-Planck Institute for Aeronomy (1P), NASA/JPL (19P), NASA/JPL/Univ. of Washington (81P), and NASA/JPL/Univ. of Maryland (9P).

primitive. The coma images of Wild 2 also show numerous jets but they have not yet been identified clearly with surface features.

The highest-resolution images to date are of the nucleus of Comet 9P/Tempel 1. These images reveal a complex surface morphology with strong evidence for erosional and geologic processes (*A'Hearn et al.,* 2005). There also appear to be two relatively well-defined and large impact craters on the surface, somewhat surprising since it was assumed that impacts were rare on such a small body, and that sublimation would quickly erode such features. Apparent layering in the surface images may be primitive, but more likely is further evidence of erosional processes acting on the nucleus. Also, there are features that suggest material flowing across the nucleus surface, in particular flowing "downhill" (*Veverka et al.,* 2006). Some surface features on Tempel 1 resemble those on Borrelly and this may be consistent with both nuclei being older and more evolved, having had a long residence time in the terrestrial planet zone.

5. COMPOSITIONAL IMPLICATIONS FOR KUIPER BELT OBJECTS FROM COMETARY OBSERVATIONS

As discussed in the chapter by Barucci et al., optical and near-infrared spectroscopy of KBOs has provided important information on their composition. Decades of studies of JFCs have produced a vast body of knowledge on their chemical makeup, giving valuable insights into (at least) kilometer-sized KBOs. Sublimation of volatiles on the surface of a JFC nucleus leads to an unbound gas and dust coma where the gas pressure gradient lifts once-embedded dust grains from the surface. The gas and dust decouple beyond distances of ~10^3 km and hence the coma appears collisionless and freely expanding to the majority of ground-based observations.

Historically the gas-phase coma has been studied via optical and near-UV spectroscopy, where molecules such as OH, C_2, C_3, and CN have bright emission bands due to resonance fluoresence with solar radiation. However, these are all at least secondary daughter species created by photodissociation and other processes from their parent molecules (i.e., $H_2O \rightarrow OH + H$), and in turn are destroyed by the same processes (i.e., $OH \rightarrow O + H$), so knowledge of the various creation and destruction pathways are necessary to accurately deduce the original sublimation rate at the nucleus. Parent molecules released directly from the nucleus such as H_2O, CO, CH_3OH, C_2H_6 (ethane), CH_4 (methane), and HCN (hydrogen cyanide) can now be observed in bright comets with high-resolution radio or near-infrared spectroscopy from the ground. Finally, the opening up of the submillimeter spectrum has allowed a large number of carbon- and sulfur-based molecules to be detected. The list of detected species, the transitions involved, and their relative abundances are given in the comprehensive review of *Bockelée-Morvan et al.* (2004). All comets studied have been shown to possess H_2O as their dominant volatile constituent; CO and CO_2 have relative abundances of ~5–20% and all other species have abundances of $X/H_2O \leq 1\%$, with the possible exception of CH_3OH (methanol).

5.1. Molecular Abundances

Although many comets appear to share similiar compositions, the existence of comets with anomalous abundance ratios of trace species has long been known, e.g., 21P/Giacobinni-Zinner (*Cochran and Barker,* 1987). The largest population study performed to date has been by *A'Hearn et al.* (1995), who used narrowband optical photometry to measure sublimation rates for several gas-phase species in 85 comets. One of their most surprising findings was that 30% of comets they observed were highly depleted (by a factor ~5) in the carbon-chain molecules C_2 and C_3. Importantly, nearly all these depleted comets were JFCs and in fact accounted for ~50% of the observed JFCs. *Fink and Hicks* (1996) obtained gaseous productions rates for 21 comets via optical spectrophotometry, and upper limits for another 18. In their sample of seven JFCs they found two to be depleted in CN and C_2. Importantly, both studies agreed on whether individual comets were "typical" or "depleted." Additionally, the *A'Hearn et al.* (1995) analysis also hinted at other possible chemically distinct groupings, including comets with enhanced C_2 and C_3 and another group with high NH/OH abundances.

A'Hearn et al. argued for this being a primordial signature, from which one concludes that there must have been at least two chemically distinct regions in the Kuiper belt during formation. They speculated that this may mark a radial distance in the protoplanetary disk, where beyond a certain distance either the creation of the parents of carbon-chain molecules was inhibited due to some process, or perhaps they were destroyed due to an increasing flux of cosmic rays. However, any interpretation must now also take into account current thinking that many JFCs may have derived from the SDO population and thus originated in the Uranus-Neptune zone. Therefore, there may be considerable overlap between the formation zones of LPCs and JFCs, which potentially confounds the explanation as to why there is such large compositional variation in just the JFCs. Furthermore, *Fink and Hicks* (1996) found carbon-chain depletions for the LPC C/1988 Y1 Yanaka, while *A'Hearn et al.* (1995) also measured depletions in the LPC C/1986 V1 Sorrels and the HTC C/1984 U2 Shoemaker. An additional point is that these studies both looked at the photodissociative carbon daughter products in the coma, and it is not clear how to accurately map these depletions onto parent molecules. However, the first comparative study of parent species in 24 comets was reported by *Biver et al.* (2003) using millimeter and submillimeter observations. They found that H_2O/HCN varied by a factor of 3 within their sample, while ratios of other carbon carrying species varied by fac-

tors of 5 to at least 9. While this is on the same order as that obtained from the optical studies above, Biver et al. did not find any clear correlation with orbital classification. Hence it now appears that a similar chemical diversity is present in JFCs, HTCs, and LPCs.

An important point that should not be overlooked is that the JFCs found to be "carbon-normal" shared similar abundances with the majority of HTCs and LPCs, implying that LPC abundances may be applicable to JFCs to first order. This is important as the majority of detailed groundbased studies are of bright HTCs or LPCs (1P/Halley, C/1996 B2 Hyakutake, C/1995 O1 Hale-Bopp). Current dynamical theories imply that LPCs formed closer to the Sun than KBOs in the region of Jupiter-Neptune over a prolonged period (*Dones et al.,* 2004). The higher temperatures and densities in this region may have produced bodies with lower volatile abundances compared to the Kuiper belt, and differences between LPCs and JFCs could be expected. The studies performed to date imply that any such differences are not striking and are less than the variations observed from comet to comet.

Studies of JFCs can also address the question of the internal heterogeneity of comets. As pointed out by *A'Hearn et al.* (1995), the similar molecular abundance ratios implies comets share the same global compositions on the largest scales (0.1–10 km). Jupiter-family comets have a known tendency to fragment and break apart, thereby allowing ices in the deep interior to sublimate (*Boehnhardt,* 2004). Molecular abundances in the combined coma of these split comets have shown no significant differences from measurements before the disruption event, also implying large-scale homogeneity within the nucleus. Recently, *Villanueva et al.* (2006) and *Dello Russo et al.* (2006) performed a detailed study using high-resolution near-IR spectoscopy of components B and C of 73P/Schwassmann-Wachmann 3 and found both components to share a C-depleted composition. This agreed with optical observations of C_2 obtained by *Schleicher* (2006).

While comets may be regarded as globally homogeneous, there exists some evidence for small-scale chemical variations within cometary nuclei. *A'Hearn et al.* (1985) observed that the outgassing rate of water on 2P/Encke varied in a different manner to other observed species, and suggested this was due to different volatile compositions at two primary sublimation sites. Intriguingly, *Lowry and Weissman* (2007) reported what appeared to be a significant variation with rotation in the optical color of Comet Encke's nucleus, which could be related to chemically distinct units on the surface. In their population study, *A'Hearn et al.* (1995) found that several other comets exhibited a change in their C-X/OH abundance ratio as a function of orbital position, implying that different vents have different relative amounts of carbon-based species. Unfortunately, their data was not dense enough to allow a search for rotationally driven variations. *Mumma et al.* (1993) reported that the detections of H_2CO in 1P/Halley appeared to be periodic, implying that production was concentrated at a single location on the rotating nucleus, although it was not possible to confirm this. Finally, *in situ* spectra of the near-nucleus coma of 9P/Tempel 1 from the Deep Impact spacecraft appeared to show a significant difference in the CO_2/H_2O gas abundance ratio on alternate sides of the nucleus (*Feaga et al.,* 2006), although further modeling of optical depth effects is required.

To summarize, it is probable that the Kuiper belt possesses two chemically distinct populations, one having depleted abundances of carbon-chain molecules with respect to HTCs and LPCs. Other chemically similar groupings also probably exist. Within these groups, there is significant evidence of small-scale chemical inhomogeneities within comets. One should therefore expect that KBOs will also exhibit localized variations in their compositions, as well as differences from object to object.

5.2. Noble Gases, Ortho-Para Ratios, and Formation Temperatures

Detection of noble gases (He, Ne, Ar) in JFCs would provide a direct link to their formation sites, as these species are chemically inert and highly volatile. Assuming a solar composition throughout the protosolar nebula, significant depletions will occur above a threshold temperature. With a model nebula, measured abundances of these species could suggest the heliocentric distance at which they formed. Unfortunately, there is yet to be a single detection of Ar or Ne in a JFC; indeed a study of three LPCs by *Weaver et al.* (2002) only produced upper limits, implying formation temperatures of ≥40–60 K. The single reported detection of Ar/O was in Hale-Bopp by *Stern et al.* (2000), where a marginal detection gave an enrichment over solar abundances of a factor of 1.8, implying that the core of Hale-Bopp has never risen above 40 K, although the measurement uncertainties were also consistent with a solar abundance. Given the unusual brightness and activity of this comet, it is likely that JFC noble gas abundances will require *in situ* measurements as planned with the Rosetta mission (*Slater et al.,* 2001).

Molecules containing two H atoms can have their nuclear spins parallel or orthogonal. The relative populations are set by the statistical weights of the levels and the excitation temperature at formation. Observations of ortho-para ratios of H_2O in Comet 103P/Hartley 2 with the Infrared Space Observatory by *Crovisier et al.* (1999) corresponded to a spin temperature of 36 ± 3 K. Values for LPCs from observations of H_2O and NH_2 range from >50 K for C/1986 P1 Wilson (*Mumma et al.,* 1993) to 28 K for C/1995 O1 Hale-Bopp (*Crovisier et al.,* 1997). *Kawakita et al.* (2001) showed that it was possible to use the relatively bright optical lines of NH_2 to derive the ortho-para ratio of the parent NH_3 to high precision. As summarized by *Bockelée-Morvan et al.* (2004), these cold temperatures imply that no re-equilibrium occurs in the nucleus, as they are consistent with heliocentric distances >50 AU. If they are primordial, these temperatures are an indication that ice formation took place in the solid phase on the surfaces of interstellar dust grains in the interstellar medium rather than in the gas phase. This para-

digm supports the viewpoint that JFCs and KBOs manage to retain signatures of their formation environment even through their subsequent dynamical and physical evolution (*Stern,* 2003), although some uncertainties remain over whether ortho-para ratios remain unchanged over 4.5 b.y.

5.3. Dust-Phase Abundances

Mid-infrared spectroscopy of cometary dust particles over the years have shown that many comets exhibit distinct emission features due to silicate grains, so one should expect the presence of silicates on the surfaces of KBOs as well. Detailed spectra of Comet C/1995 O1 (Hale-Bopp) obtained by *Crovisier et al.* (1997) with the European Space Agency (ESA) Infrared Space Observatory revealed the presence of crystalline Mg-rich olivine and pyroxene, together with amorphous pyroxene. Spectra of the ejecta from the Deep Impact encounter with 9P/Tempel 1 were obtained by *Lisse et al.* (2006) using the Spitzer Space Telescope. Apart from containing similar minerals to Hale-Bopp, spectral fitting also revealed the presence of crystalline Fe-rich olivines and pyroxenes, together with phyllosillicates, carbonates, polyaromatic hydrocarbons (PAHs), and amorphous carbon. Lisse et al. conclude that carbonaceous material makes up ~15% of the observed dust, less than that found for other comets but consistent with the classification of 9P/Tempel 1 as a carbon-depleted comet.

In situ sampling of cometary dust particles by the ESA Giotto spacecraft and the two Soviet Vega spacecraft at 1P/Halley revealed a large population of organic dust particles composed primarily of H, C, N, and O (*Fomenkova et al.,* 1992). At Halley these "CHON" grains formed ~25% of the dust particles detected, while 50% were a mixture of CHON and silicate grains. The presence of dust grains containing large amounts of volatiles is also implied by the observation of distributed sources of CN, CO, and OCS in the inner comae of several comets. Hence cometary dust grains have been shown to contain material from high-temperature and low-temperature environments, implying that KBOs formed in a well-mixed environment. Furthermore, at the time of writing, results of the analysis of dust particles captured by the NASA Stardust sample-return mission (*Brownlee et al.,* 2004) became available. One of the many highlights was that Comet 81P/Wild 2 contains material formed at high temperature in the inner solar system. Therefore, if this comet accreted in the colder Kuiper belt region then this material must have been transported there, consistent with several protosolar disk models (see *McKeegan et al.,* 2006).

5.4. Nucleus Spectroscopy

Ground-based spectroscopy of cometary nuclei have not yet revealed any spectral signatures (*Lamy et al.,* 2004). In the past this was possibly due to their extreme faintness in the near-IR where ice absorption bands lie. However, the discovery by current near-Earth object surveys of JFCs with weak or intermittent outgassing at small heliocentric distances now allows more detailed studies. High signal-to-noise near-infrared spectra of 162P/Siding-Spring obtained by *Campins et al.* (2006) showed no sign of any absorption bands with depths >2% of the continuum. A similar null result was obtained for C/2001 OG108 by *Abell et al.* (2005). This is possibly understandable as these are weakly active comets, which implies that their surfaces are heavily mantled by dust particles, but it is still disappointing.

Spectroscopy of resolved nuclei by spacecraft have been more successful. Spectroscopy with Deep Space 1 observed an absorption band at 2.39 μm on the surface of 19P/Borrelly, whose origin is currently unknown. Three areas exhibiting water-ice absorption bands at 1.5 μm and 2.0 μm were identified on the nucleus of 9P/Tempel 1 with the Deep Impact spacecraft (*Sunshine et al.,* 2006). These covered an extremely small fraction of the visible surface area, and remote disk-integrated spectra would not have revealed them. If other JFCs share similar surface characteristics, it is not surprising that ground-based spectroscopy efforts have been unsuccessful. Of course, JFCs will have undergone substantial erosion and alteration of their surfaces through sublimation processes (*Meech and Svoren,* 2004), so it is probably unwise to attempt comparisons with the extant spectra of the much larger and less eroded KBOs.

6. DISCUSSION

Throughout this chapter we have shown that studying certain aspects of JFC nuclei and their comae can reveal information on the bulk physical properties of small KBOs, and their composition, and just as importantly what cannot be learned. The size distribution of JFCs is particularly valuable for ascertaining the KBO size distribution at the small km-size end. Although the various size distribution estimates have not yet converged on a single solution, we can say for sure that the JFC size distribution is much shallower than for the KBOs measured at the much larger (>100 km) size regime. As pointed out by *Lowry et al.* (2003), this could imply that there is some process acting on cometary nuclei that is significantly altering the size distribution. For example, the rate of complete disintegration of small nuclei could be more frequent than once thought (i.e. smaller objects are being removed from the system, which could reduce the slope's steepness). Alternatively, there is a broken power law to the size distribution within the belt. A record is preserved of this within the JFCs, as surface sublimation does not significantly affect the size distribution as the small KBOs evolve inwards through the planetary region. This broken power law will need to be accounted for in any models of the formation and evolution within the Kuiper belt.

Studying the rotational properties of JFCs and KBOs is also very revealing and indicates the presence of a spin-period or density cut-off which naturally has implications for the internal structure of KBOs. It is likely that internal properties are preserved within the nuclei of JFCs as they evolve dynamically. Therefore the spin period cut-off should be common to both groups, which we believe it is although

statistics are small. If such a spin-period cut-off is unambiguously confirmed then this would act as a *physical link* to KBOs, supporting the established dynamical links. Although we can infer KBO compositional information from cometary observations, as discussed in section 5, establishing compositional links are still in their early stages. Of course, an obvious caveat to this and the arguments above is that many JFCs may have originated from within the giant planets region. Awaiting investigation are the isotopic ratios in JFCs, for which no remote observations yet exist. The first preliminary measurements have recently been reported for dust particles collected *in situ* by the Stardust mission (*McKeegan et al.,* 2006).

It is now widely accepted from both the early and latest observations that surface colors and albedos of comets do not reflect the surface properties of KBOs, perhaps due to surface sublimation and mantle formation processes acting on JFCs, and one must proceed with caution when making comparisons. Of course, we learn a great deal about how JFC surfaces are evolving as they migrate to the planetary region. The search for possible color-color groupings within the JFC population will go on. As for albedo, systematic surveys of JFCs (as well as Centaurs and KBOs) using the recently launched Spitzer Infrared Space Telescope will allow their size and albedo distributions to be constrained with much superior accuracy, hopefully allowing comet-nucleus observers to reach a consensus on the JFC size-distribution slope.

Close-up spacecraft images reveal details on the likely internal structure, such as the presence of large boulders protruding through the surface of Comet 81P/Wild 2, and the binary appearance of Comet 19P/Borrelly, both supporting the rubble-pile model for the internal structure of JFCs (*Weissman,* 1986), and thus the KBOs. The very detailed images from Deep Impact show evidence of material "flowing" on the surface of comet 9P/Tempel 1.

The next spacecraft mission to a JFC nucleus is the Rosetta mission by the ESA (*Schwehm,* 2003). Not only will the nucleus of 67P/Churyumov-Gerasimenko be imaged in fine detail with the OSIRIS optical imaging camera (*Keller et al.,* 2007), but the evolution of surface features will be monitored for ~1 yr. Of the many questions this mission will answer, some that are obviously relevant to this discussion will be the first highly accurate density measurement for a cometary nucleus. Also, if similar material flows are seen, one could look for changes in their structure to assess if they are being produced today, thus increasing their likelihood of occurring on KBO surfaces. We look forward to seeing if these details are reproduced on the surfaces of KBOs when the New Horizons probe goes on to explore the Kuiper belt after its main mission at the Pluto and Charon system (see chapter by Weaver and Stern), and seeing how a "fresh" JFC should look.

Acknowledgments. We thank J. Crovisier and an anonymous referee for their very helpful reviews. We gratefully acknowledge support from the Leverhulme Trust (S.C.L.) and the UK Particle Physics and Astronomy Research Council (S.C.L., A.F.). This work was performed in part at the Jet Propulsion Laboratory under a contract with NASA, and partly funded by the NASA Rosetta and Planetary Astronomy Programs (P.R.W.).

REFERENCES

Abell P. A., Fernández Y. R., Pravec P., French L. M., Farnham T. L., et al. (2005) Physical characteristics of comet nucleus C/2001 OG108 (LONEOS). *Icarus, 179,* 174–194.

A'Hearn M. F., Birch P. V., Feldman P. D., and Millis R. L. (1985) Comet Encke: Gas production and lightcurve. *Icarus, 64,* 1–10.

A'Hearn M. F., Millis R. L., Schleicher D. G., Osip D. J., and Birch P. V. (1995) The ensemble properties of comets: Results from narrowband photometry of 85 comets, 1976–1992. *Icarus, 118,* 223–270.

A'Hearn M. F., Belton M. J. S., Delamere W. A., Kissel J., Klaasen K. P., et al. (2005) Deep Impact: Excavating Comet Tempel 1. *Science, 310,* 258–264.

Asphaug E., Ryan E. V., and Zuber M. T. (2002) Asteroid interiors. In *Asteroids III* (W. F. Bottke Jr. et al., eds.), pp. 463–484. Univ. of Arizona, Tucson.

Barucci M. A., Belskaya I. N., Fulchignoni M., and Birlan M. (2005) Taxonomy of Centaurs and trans-neptunian objects. *Astron. J., 130,* 1291–1298.

Bauer J. M., Meech K. J., Fernández Y. R., Pittichova J., Hainaut O. R., Boehnhardt H., and Delsanti A. C. (2003) Physical survey of 24 Centaurs with visible photometry. *Icarus, 166,* 195–211.

Bernstein G. M., Trilling D. E., Allen R. L., Brown M. E., Holman M., and Malhotra R. (2004) The size distribution of trans-Neptunian bodies. *Astron. J., 128,* 1364–1390.

Biver N., Bockelée-Morvan D., Crovisier J., Colom P., Henry F., Moreno R., Paubert G., Despois D., and Lis D. C. (2003) Chemical composition diversity among 24 comets observed at radio wavelengths. *Earth Moon Planets, 90,* 323–333.

Bockelée-Morvan D., Crovisier J., Mumma M. J., and Weaver H. A. (2004) The composition of cometary volatiles. In *Comets II* (M. C. Festou et al., eds.), pp. 391–423. Univ. of Arizona, Tucson.

Boehnhardt H. (2004) Split comets. In *Comets II* (M. C. Festou et al., eds.), pp. 301–316. Univ. of Arizona, Tucson.

Brownlee D. E., Horz F., Newburn R. L., Zolensky M., Duxbury T. C., et al. (2004) Surface of young Jupiter family Comet 81P/Wild 2: View from the Stardust spacecraft. *Science, 304,* 1764–1769.

Campins H., Ziffer J., Licandro J., Pinilla-Alonso N., Fernandez Y., de León J., Mothé-Diniz T., and Binzel R. P. (2006) Nuclear spectra of Comet 162P/Siding Spring (2004 TU12). *Astron J., 132,* 1346–1353.

Crovisier J., Leech K., Bockelée-Morvan D., Brooke T. Y., Hanner M. S., Altieri B., Keller H. U., and Lellouch E. (1997) The spectrum of Comet Hale-Bopp (C/1995 01) observed with the Infrared Space Observatory at 2.9 AU from the Sun. *Science, 275,* 1904–1907.

Crovisier J., Encrenaz T., Lellouch E., Bockelée-Morvan D., Altieri B., et al. (1999) ISO spectroscopic observations of short-period comets. In *The Universe as Seen by ISO* (P. Cox and M. F. Kessler, eds.), p. 161. ESA SP-427, Noordwijk, The Netherlands.

Dello Russo N., Vervack R. J. Jr., Weaver H. A., Biver N., Bockelée-Morvan D., Crovisier J., and Lisse C. M. (2006) High-

resolution infrared spectroscopy of Comet 73P/Schwassmann-Wachmann 3: A test for chemical heterogeneity within a cometary nucleus (abstract). *Bull. Am. Astron. Soc., 38,* #03.05.

Delsante A., Hainaut O., Jourdeuil E., Meech K. J., Boehnhardt H., and Barrera L. (2004) Simultaneous visible-near IR photometric study of Kuiper belt object surfaces with the ESO/Very Large Telescopes. *Astron. Astrophys., 417,* 1145–1158.

Dohnanyi J. W. (1969) Collisional models of asteroids and their debris. *J. Geophys. Res., 74,* 2531–2554.

Dones L., Weismann P. R., Levison H. F., and Duncan M. J. (2004) Oort cloud formation and dynamics. In *Comets II* (M. C. Festou et al., eds.), pp. 153–174. Univ. of Arizona, Tucson.

Doressoundiram A., Peixinho N., Doucet C., Mousis O., Barucci A. M., Petit J. M., and Veillet C. (2005) The Meudon Multicolour Survey (2MS) of Centaurs and trans-neptunian objects: Extended dataset and status on the correlations reported. *Icarus, 174,* 90–104.

Duncan M. and Levison H. F. (1997) A scattered comet disk and the origin of Jupiter-family comets. *Science, 276,* 1670–1672.

Duncan M., Levison H., and Dones L. (2004) Dynamical evolution of ecliptic comets. In *Comets II* (M. C. Festou et al., eds.), pp. 193–204. Univ. of Arizona, Tucson.

Farinella P. and Davis D. R. (1996) Short-period comets: Primordial bodies or collisional fragments? *Science, 273,* 938–941.

Feaga L. M., A'Hearn M. F., Sunshine J. M., Groussin O., and the Deep Impact Science Team (2006) Asymmetry of gaseous CO_2 and H_2O in the inner coma of Comet Tempel 1 (abstract). In *Lunar and Planetary Science XXXVII,* Abstract #2149. Lunar and Planetary Institute, Houston (CD-ROM).

Fernández J. A., Tancredi G., Rickman H., and Licandro J. (1999) The population, magnitudes, and sizes of Jupiter family comets. *Astron. Astrophys., 352,* 327–340.

Fernández Y. R., Jewitt D. C., and Sheppard S. S. (2001) Low albedos among extinct comet candidates. *Astrophys. J. Lett., 553,* L197–L200.

Fernández Y. R., Campins H., Kassis M., Hergenrother C. W., Binzel R. P., Licandro J., Hora J. L., and Adams J. D. (2006) Comet 162P/Siding Spring: A surprisingly large nucleus. *Astrophys. J., 132,* 1354–1360.

Fink U. and Hicks M. D. (1996) A survey of 39 comets using CCD spectroscopy. *Astrophys. J., 459,* 729–743.

Fomenkova M., Kerridge J. F., Marti K., and McFadden L. (1992) Classification of carbonaceous components in Comet Halley CHON particles (abstract). In *Lunar and Planetary Science XXIII,* p. 379. Lunar and Planetary Institute, Houston.

Fulchignoni M., Barucci M. A., Belskaya I., and Doressoundiram A. (2006) TNOs' taxonomy confirmed (abstract). *Bull. Am. Astron. Soc., 38,* #40.05.

Gladman B., Kavelaars J. J., Petit J.-M., Morbidelli A., Holman M. J., and Loredo T. (2001) The structure of the Kuiper belt: Size distribution and radial extent. *Astron. J., 122,* 1051–1066.

Grundy W. M., Noll K. S., and Stephens D. C. (2005) Diverse albedos of small trans-neptunian objects. *Icarus, 176,* 184–191.

Hainaut O. and Delsanti A. C. (2002) Colors of minor bodies in the outer solar system. A statistical analysis. *Astron. Astrophys., 389,* 641–664.

Holsapple K. A. (2003) Could fast rotator asteroids be rubble piles? (abstract). In *Lunar and Planetary Science XXXIV,* Abstract #1792. Lunar and Planetary Institute, Houston (CD-ROM).

Horner J., Evans N. W., and Bailey M. E. (2004) Simulations of the population of Centaurs — I. The bulk statistics. *Mon. Not. R. Astron. Soc., 354,* 798–810.

Hsieh H. H. and Jewitt D. (2006) A population of comets in the main asteroid belt. *Science, 312,* 561–563.

Jewitt D. C. (2002) From Kuiper Belt object to cometary nucleus: The missing ultrared matter. *Astron. J., 123,* 1039–1049.

Jewitt D. and Luu J. (1993) Discovery of the candidate Kuiper belt object 1992 QB1. *Nature, 362,* 730–732.

Jewitt D. C. and Luu J. X. (2001) Colors and spectra of Kuiper belt objects. *Astron. J., 122,* 2099–2114.

Kawakita H., Watanabe J.-I., Ando H., Aoki W., Fuse T., et al. (2001) The spin temperature of NH_3 in comet C/1994 S4 (LINEAR). *Science, 294,* 1089–1091.

Keller H. U., Arpigny C., Barbieri C., Bonnet R. M., Cazes S., et al. (1986) First Halley multicolour camera imaging results from Giotto. *Nature, 321,* 320–326.

Keller H. U., Barbieri C., Lamy P., Rickman H., Rodrigo R., et al. (2007) OSIRIS — The Optical, Spectroscopic, and Infrared Remote Imaging System. *Space Sci. Rev., 128,* 433–506.

Lacerda P. and Luu J. X. (2006) Analysis of the rotational properties of Kuiper belt objects. *Astron. J., 131,* 2314–2326.

Lamy P. L. and Toth I. (2005) The colors of cometary nuclei and other primitive bodies (abstract). In *IAU Symposium No. 229: Asteroids, Comets, Meteors,* August 7–12, 2005, Rio de Janeiro, Brazil.

Lamy P. L., Toth I., A'Hearn M. F., Weaver H. A., and Weissman P. R. (2001) Hubble Space Telescope observations of the nucleus of Comet 9P/Tempel 1. *Icarus, 154,* 337–344.

Lamy P. L., Toth I., Fernández Y. R., and Weaver H. A. (2004) The sizes, shapes, albedos, and colours of cometary nuclei. In *Comets II* (M. C. Festou et al., eds.), pp. 223–264. Univ. of Arizona, Tucson.

Levison H. and Duncan M. (1994) The long-term dynamical behavior of short-period comets. *Icarus, 108,* 18–36.

Lisse C. M., Van Cleave J., Adams A. C., A'Hearn M. F., Fernández Y. R., et al. (2006) Spitzer spectral observations of the Deep Impact ejecta. *Science, 313,* 635–640.

Lowry S. C. and Weissman P. R. (2007) Rotation and color properties of the nucleus of Comet 2P/Encke. *Icarus, 188,* 212–223.

Lowry S. C., Fitzsimmons A., and Collander-Brown S. (2003) CCD photometry of distant comets III: Ensemble properties of Jupiter family comets. *Astron. Astrophys., 397,* 329–343.

Lowry S. C., Fitzsimmons A., Pravec P., Vokrouhlický D., Boehnhardt H., Taylor P. A., Margot J-L., Galád A., Irwin M., Irwin J., and Kušnirák P. (2007) Direct detection of the asteroidal YORP effect (abstract). In *Lunar and Planetary Science XXXVIII,* Abstract #2438. Lunar and Planetary Institute, Houston (CD-ROM).

Luu J. X. (1993) Spectral diversity among the nuclei of comets. *Icarus, 104,* 138–148.

Luu J. X. and Jewitt D. C. (1992) Near-aphelion CCD photometry of Comet P/S Schwassmann-Wachmann 2. *Astron. J., 104,* 2243–2249.

McKeegan D., Aléon J., Bradley J., Brownlee D., Busemann H., et al. (2006) Isotopic compositions of cometary matter returned by Stardust. *Science, 314,* 1724–1728.

Meech K. J. and Svoren J. (2004) Using cometary activity to trace the physical and chemical evolution of cometary nuclei. In *Comets II* (M. C. Festou et al., eds.), pp. 223–264. Univ. of Arizona, Tucson.

Meech K. J., Hainaut O. R., and Marsden B. G. (2004) Comet nucleus size distribution from HST and Keck telescopes. *Icarus, 170,* 463–491.

Mumma M. J., Weissman P. R., and Stern S. A. (1993) Comets

and the origin of the solar system: Reading the Rosetta Stone. In *Protostars and Planets III* (E. H. Levy and J. I. Lunine, eds.), pp. 1177–1252. Univ. of Arizona, Tucson.

O'Brien D. P. and Greenberg R. (2003) Steady-state size distributions for collisional populations: Analytical solution with size dependent strength. *Icarus, 164,* 334–345.

Ortiz J. L., Gutiérrez P. J., Santos-Sanz P., Casanova V., and Sota A. (2006) Short-term rotational variability of eight KBOs from Sierra Nevada Observatory. *Astron. Astrophys., 447,* 1131–1144.

Peixinho N., Doressoundiram A., Delsanti A., Boehnhardt H., Barucci M. A., and Belskaya I. (2003) Reopening the TNOs color controversy: Centaurs bimodality and TNOs unimodality. *Astron. Astrophys., 410,* L29–L32.

Peixinho N., Boehnhardt H., Belskaya I., Doressoundiram A., Barucci M. A., and Delsanti A. C. (2004) ESO Large Program on Centaurs and KBOs: Visible colours — Final results. *Icarus, 170,* 153–166.

Pravec P., Harris A. W., and Michalowski T. (2002) Asteroid rotations. In *Asteroids III* (W. F. Bottke Jr. et al., eds.), pp. 113–122. Univ. of Arizona, Tucson.

Rabinowitz D. L., Barkume K., Brown M. E., Roe H., Schwartz M., Tourtellotte S., and Trujillo C. (2006) Photometric observations constraining the size, shape, and albedo of 2003 EL61, a rapidly rotating, Pluto-sized object in the Kuiper belt. *Astrophys. J., 639,* 1238–1251.

Rubincam D. P. (2000) Radiative spin-up and spin-down on small asteroids. *Icarus, 148,* 2–11.

Samarasinha N.H., Mueller B. E. A., Belton M. J. S., and Jorda L. (2004) Rotation of cometary nuclei. In *Comets II* (M. C. Festou et al., eds.), pp. 281–299. Univ. of Arizona, Tucson.

Schleicher D. (2006) Comet 73P/Schwassmann-Wachmann. *IAU Circular 8681.*

Schwehm G. (2003) The Rosetta mission — The new mission scenario (abstract). *Bull. Am. Astron. Soc., 35,* #41.06.

Sheppard S. S., Jewitt D. C., Trujillo C. A., Brown M. J. I., and Ashley M. C. B. (2000) A wide-field CCD survey for Centaurs and Kuiper belt objects. *Astron. J., 120,* 2687–2694.

Slater D. C., Stern S. A., Booker T., Scherrer J., A'Hearn M. F., Bertaux J.-L., Feldman P. D., Festou M. C., and Siegmund O. H. (2001) Radiometric and calibration performance of the Rosetta UV imaging spectrometer ALICE. In *UV/EUV and Visible Space Instrumentation for Astronomy and Solar Physics* (O. H. W. Siegmund et al., eds.), pp. 239–247. Proc. SPIE Vol. 4498.

Snodgrass C. (2006) Forms and rotational states of the nuclei of ecliptic comets. Ph.D. thesis, Queen's Univ. Belfast.

Soderblom L. A., Becker T. L., Bennett G., Boice D. C., Britt D. T., et al. (2002) Observations of Comet 19P/Borrelly by the Miniature Integrated Camera and Spectrometer aboard Deep Space 1. *Science, 296,* 1087–1091.

Stern S. A. (1995) Collisional time scales in the Kuiper disk and their implications. *Astron. J., 110,* 856–868.

Stern S. A. (2003) The evolution of comets in the Oort cloud and Kuiper belt. *Nature, 426,* 639–642.

Stern S. A., Slater D. C., Festou M. C., Parker J. Wm., Gladstone G. R., A'Hearn M. F., and Wilkinson E. (2000) The discovery of argon in Comet C/1995 O1 (Hale-Bopp). *Astrophys. J. Lett., 544,* L169–L172.

Stuart J. S. (2001) A near-Earth asteroid population estimate from the LINEAR survey. *Science, 294,* 1691–1693.

Sunshine J. M., A'Hearn M. F., Groussin O., Li J.-Y., Belton M. J. S., et al. (2006) Exposed water ice deposits on the surface of Comet 9P/Tempel 1. *Science, 311,* 1453–1455.

Tancredi G., Fernández J. A., Rickman H., and Licandro J. (2006) Nuclear magnitudes and the size distribution of Jupiter family comets. *Icarus, 182,* 527–549.

Taylor P. A., Margot J.-L., Vokrouhlický D., Scheeres D. J., Pravec P., et al. (2007) The increasing spin rate of asteroid (54509) 2000 PH5: A result of the YORP effect (abstract). In *Lunar and Planetary Science XXXVIII,* Abstract #2229. Lunar and Planetary Institute, Houston (CD-ROM).

Tegler S. C. and Romanishin W. (1998) Two distinct populations of Kuiper-belt objects. *Nature, 392,* 49–51.

Tegler S. C. and Romanishin W. (2003) Resolution of the Kuiper belt object color controversy: Two distinct color populations. *Icarus, 161,* 181–191.

Tholen D. J. (1984) Asteroid taxonomy from cluster analysis of photometry. Ph.D. thesis, Univ. of Arizona, Tucson.

Trilling D. E. and Bernstein G. M. (2006) Light curves of 20–100 km Kuiper belt objects using the Hubble Space Telescope. *Astron. J., 131,* 1149–1162.

Trujillo C. A., Jewitt D. C., and Luu J. X. (2001) Properties of the trans-Neptunian belt: Statistics from the Canada-France-Hawaii telescope survey. *Astron. J., 122,* 457–473.

Veverka J., Thomas P., and Hidy A. (2006) Tempel 1: Surface processes and the origin of smooth terrains (abstract). In *Lunar and Planetary Science XXXVII,* Abstract #1364. Lunar and Planetary Institute, Houston (CD-ROM).

Villaneuva G. L., Bobnev B. P., Mumma M. J., Magee-Sauer K., DiSanti M. A., Salyk M. A., and Blake G. A. (2006) The volatile composition of the split ecliptic Comet 73P/Schwassmann-Wachmann 3: A comparison of fragments B and C. *Astrophys. J. Lett., 650,* L87–L90.

Weaver H. A., Feldman P. D., Combi M. R., Krasnopolsky V., Lisse C. M., and Shemansky D. E. (2002) A search for argon in three comets using the Far Ultraviolet Spectroscopic Explorer. *Astrophys J. Lett., 576,* L95–L98.

Weissman P. R. (1979) Physical and dynamical evolution of long-period comets. In *Dynamics of the Solar System* (R. L. Duncabe, ed.), pp. 277–282. IAU Symposium No. 81, Reidel, Dordrecht.

Weissman P. R. (1986) Are cometary nuclei primordial rubble piles? *Nature, 320,* 242–244.

Weissman P. R. and Levison H. F. (1997) The population of the trans-Neptunian region. In *Pluto and Charon* (S. A. Stern and D. Tholen, eds.), pp. 559–604. Univ. of Arizona, Tucson.

Weissman P. R. and Lowry S. C. (2003) The size distribution of Jupiter-family cometary nuclei (abstract). In *Lunar and Planetary Science XXXIV,* Abstract #2003. Lunar and Planetary Institute, Houston (CD-ROM).

Weissman P., Doressoundiram A., Hicks M., Chamberlin A., Sykes M., Larson S., and Hergenrother C. (1999) CCD photometry of comet and asteroid targets of spacecraft missions (abstract). *Bull. Am. Astron. Soc., 31,* #31.03.

Weissman P. R., Asphaug E., and Lowry S. C. (2004) Structure and density of cometary nuclei. In *Comets II* (M. C. Festou et al., eds.), pp. 337–358. Univ. of Arizona, Tucson.